A REPORT ON THE 19 MAY 2011 KÜTAHYA-SİMAV EARTHQUAKE (PRELIMINARY REPORT)

In collaboration with
Earthquake Engineering Research Center (EERC)
Middle East Technical University, Ankara Turkey

Earthquake Research Department
Disaster Management and Emergency Presidency (AFAD), Ankara Turkey

List of Collaborators

Earthquake Engineering Research Center (EERC)
M. Abdullah Sandıkkaya
Mehtap Şenyurt
Alper Aldemir
Emre Akın
Aida Azari Sisi
Barış Binici
Erdem Canbay
Sinan Akkar

Disaster Management and Emergency Presidency (AFAD)
Ulubey Çeken
Turgay Kuru
Aytaç Apak
Derya Kökbudak
Eren Tepeuğur
Hakan Albayrak
Vedat Özsaraç
Selim Sezer
Cüneyt Şahin

REPORT NO: METU/EERC 2011-02

JUNE 2011
ANKARA

MIDDLE EAST TECHNICAL UNIVERSITY

EARTHQUAKE ENGINEERING RESEARCH CENTER

Table of Contents

Table of Figures

List of Tables

1. Introduction

An earthquake occurred on May 19, 2011 at 20:15 (GMT) in Simav, Kütahya located in the western part of Turkey. The location of earthquake is on the Yesilköy and Çavdır fault segments (Simav faulting system; Koçyiğit, 2011). The earthquake, indirectly, caused 2 casualties and injuries to 122 people. The epicentral coordinates of the earthquake are reported as 39.1328N – 29.0820E by the Earthquake Department of the Disaster and Emergency Management Presidency (DEMP). The DEMP reported the depth and magnitude of the Kütahya-Simav earthquake as 24.46 km and ML5.7, respectively. The moment tensor solution and the faulting mechanism information is also provided by the same agency. Table 1 lists the depth, magnitude, epicenter coordinates as well as the other relevant source parameters that are reported by other national and international seismic agencies. Although the magnitude information does not show significant differences between the seismic agencies, the depth information provided by DEMP is differ considerably with respect to other agencies. Figures 1-3 show the major active faulting system, the epicenter of the mainshock and the scatter of the aftershocks as well the historical events in the region. Approximately 2500 aftershocks occurred after the mainshock. The magnitude range (ML) of these aftershocks is between 1.3 and 4.8. The time dependent decay of the aftershocks is given in Figure 4.

This report presents preliminary information about the strong-motion data recorded during the mainshock as well as the structural damage observed after the earthquake. The current version of the report will be updated by extending the discussions on the recorded ground motions.

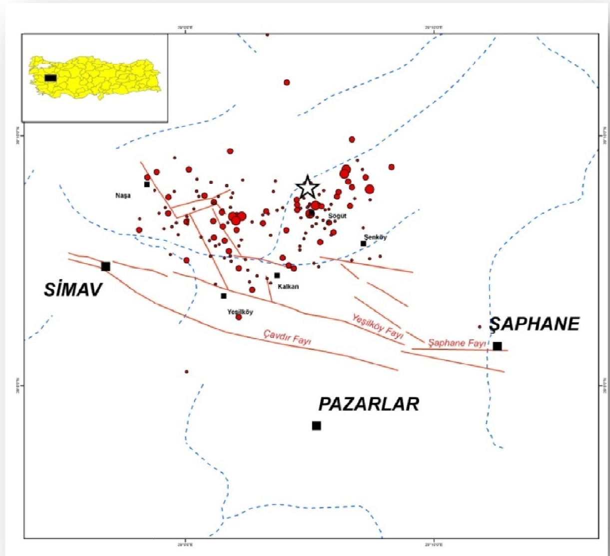

Figure 1. Major faulting system in the Simav region. The symbol star shows the epicentral coordinates of the main-shock and red circles indicate the epicentral coordinates of the aftershocks within a few days after the main event (Koçyiğit, 2011).

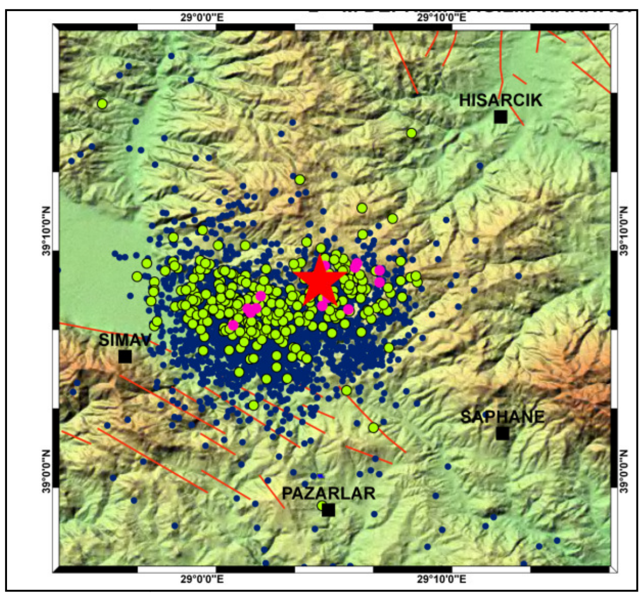

Figure 2. Major faulting system acting in the Simav region, red star shows the epicentral coordinates of the main-shock. The small dots show the epicentral coordinates of the aftershocks until June 06. (Pink, green and blue dots show the earthquakes with ML+4, ML+3, and ML+2, respectively).

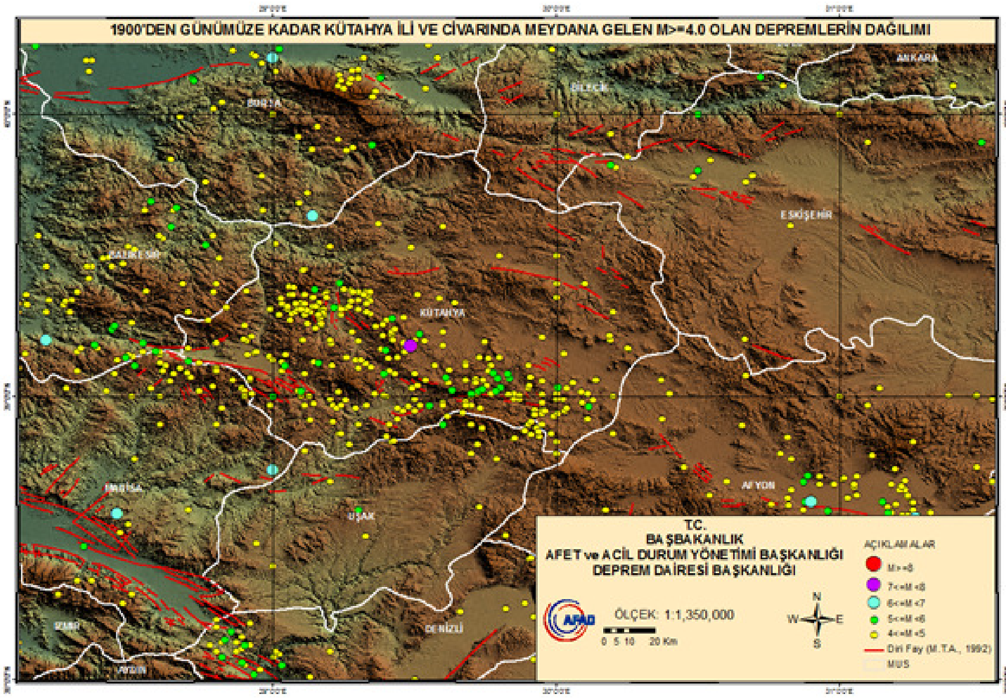

Figure 3. Historic events with M+4 from 1900s to today

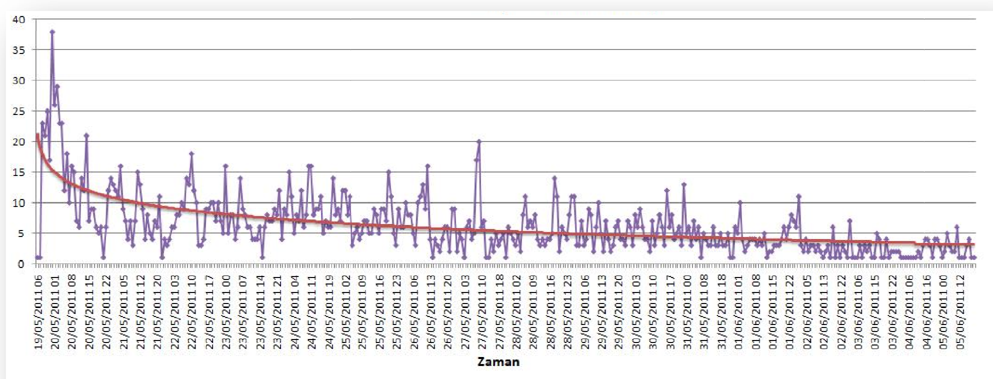

Figure 4. Time dependent decay of the after-shocks

2. Processed strong-motion

This preliminary report presents the raw and processed accelerometric data of the mainshock. In addition, the comparisons of the observed data with the recently developed ground-motion predictive models are studied. As of June 06, a total of 84 three-component recordings are available through the website http://kyh.deprem.gov.tr/ftpt.htm . Figure 5 shows the recording stations with the largest ground acceleration values. The downloaded raw recordings are firstly evaluated with the visual inspection of the data whether or not they include non-standard errors (Douglas, 2003). Then an initial baseline adjustment (zeroth-order correction) is applied to the accelerograms. If there is a pre-event buffer in the accelerograms, the mean of 90 percent of this pre-event time is removed from the entire record; if not the mean of the whole record is considered. Finally, a bi-directional, fourth-order Butterworth filter is used during the filtering process. Table 2 summarizes the low-cut and high-cut filter cut-offs determined by the procedure described in Akkar and Bommer (2006), Douglas and Boore (2011) and Akkar et al. (2011). The processing procedure is done by using the USDP software. (This software uses the public-open data processing codes of Dr. David M. Boore at USGS, Menlo Park California). The same table also lists the suggested the long-period usable period ranges of each recording based on the empirical expressions proposed in Akkar and Bommer (2006). Whenever this procedure is inapplicable, usable period is taken as 80% of the reciprocal of the low-cut filter value (Abrahamson and Silva, 1997). The processed recordings will be disseminated through the webs of METU-EERC and the strong-ground motion group of DEMP. The websites will also contain the raw accelerometric data for researchers who want to do their own data processing.

Table 3 shows the coordinates of the stations and VS30 values, if available. This table also lists the source-to-site distance metrics (R_{epi}, R_{hyp}, R_{JB} and R_{rup}) computed from the information obtained from GCMT[1]. The calculation procedure for distance metrics is described by Kaklamonos et al. (2011). The observed PGA and PGV values are compared with the estimations of the predictive models developed within the context of the Next Generation Attenuation Models project (i.e., Abrahamson and Silva (2008), Boore and Atkinson (220), Campbell and Bozorgnia (2008) and Choui and Youngs (2008)), as well the recent pan-European model of Akkar and Bommer (2010) and the recent Turkish model of Akkar and Cagnan (2010). In order to simplify the comparisons, the recordings are converted to VS30 = 760 m/s or corresponding rock definitions. Figure 6 and 7 show these comparisons.

[1] Global Centroid Moment Tensor

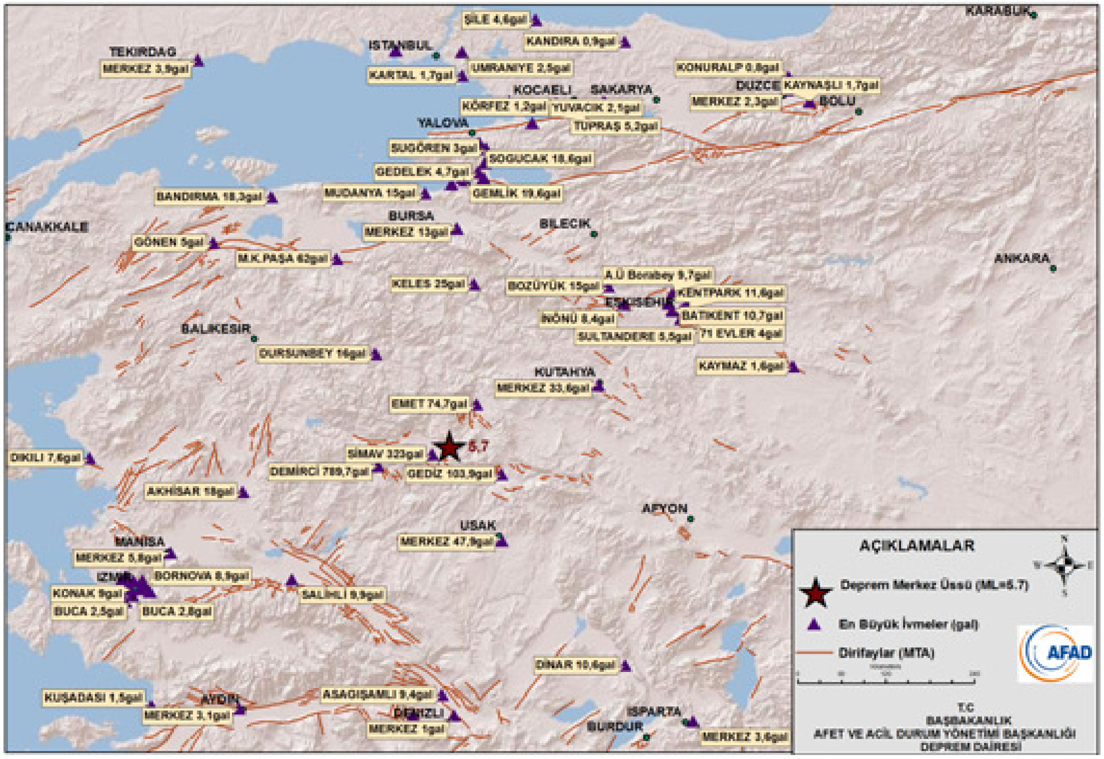

Figure 5. The distribution of the stations recorded the main-shock

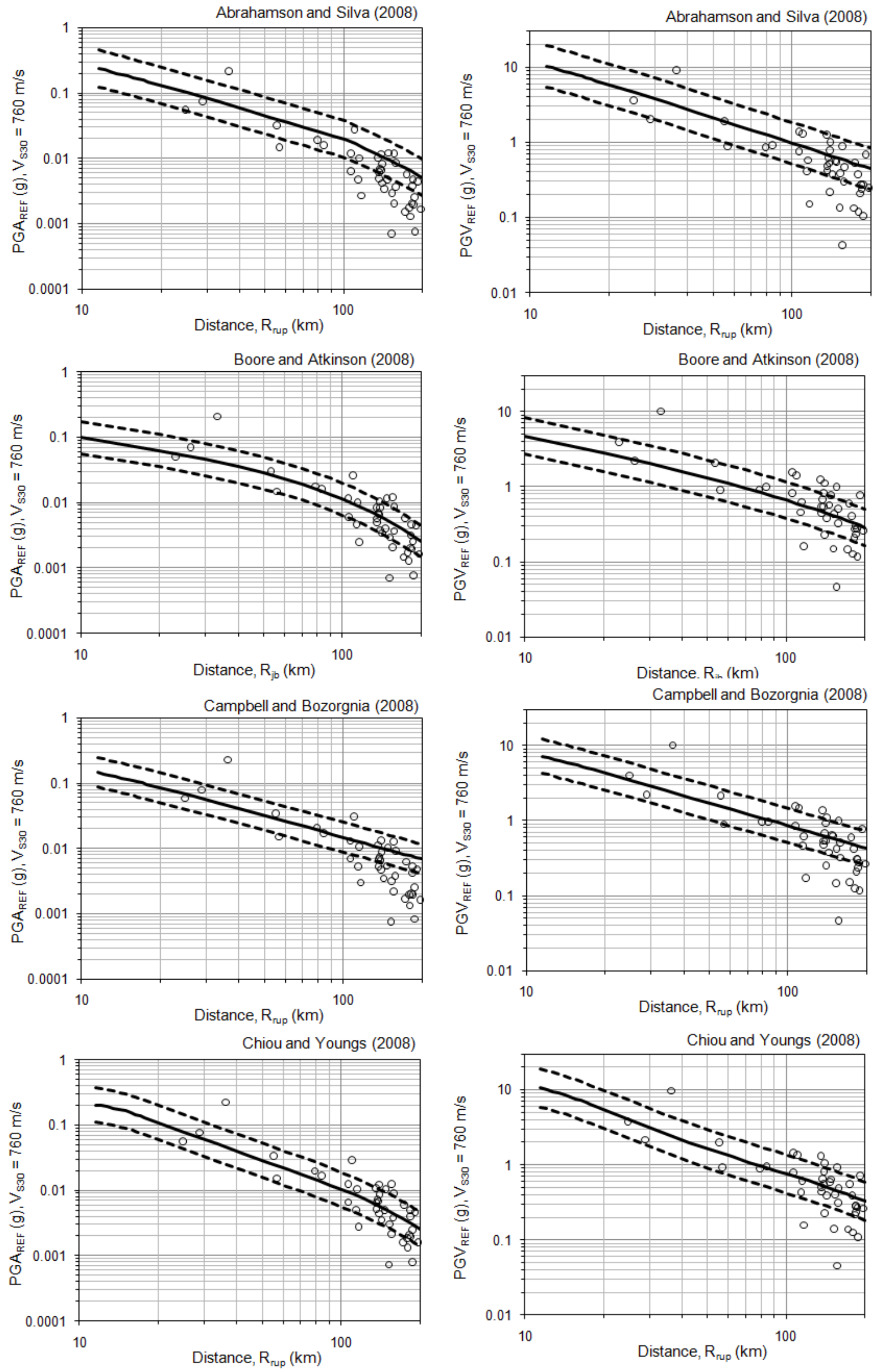

Figure 6. Comparisons of the observed data with NGA models. Left and right columns show the comparative plots for PGA and PGV, respectively.

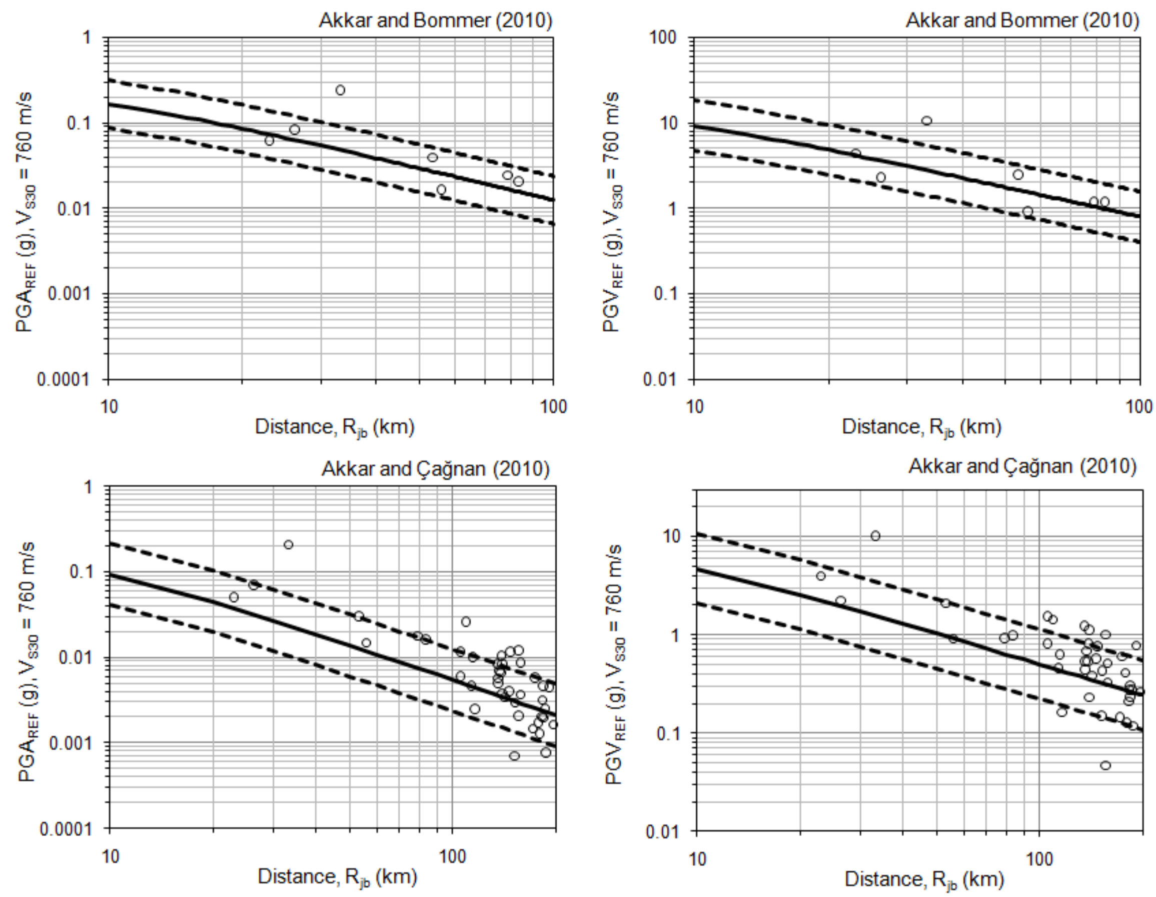

Figure 7. Comparisons of the observed data with Akkar and Bommer (2010) and Akkar and Çağnan (2010) ground-motion models. Left and right column is for PGA and PGV, respectively.

3. A special study on the Demirci record (Station Id: 4504)

Unusually high peak ground acceleration of this recording that is recorded approximately 35 km from the ruptured fault led additional analysis to investigate the nature of this high frequency peak. This accelerogram was recorded at a free-field station deployed on a slopy hill as shown in Figure 8. The shear-wave velocity profile reaches about 475 m/s at depth greater than 30m (Figure 9) and suggests that the station is deployed over a relatively soft soil deposit (VS30=336 m/s). In order to observe the frequency content of this recording, the smoothed Fourier acceleration spectra (FAS) of horizontal and vertical components are calculated by applying Konno-Omachi smoothing procedure (provided in the public-open codes of Dr. David M. Boore, USGS Menlo Park California) as shown in Figure 10. The FAS trends of the 3 components are fairly the same except for the observed peak in the EW component around 8 Hz. In order to understand the influence of this frequency component about 8 Hz, the EW component is filtered with a series of hi-cut values (30 Hz, 20 Hz, 10 Hz and 8 Hz). The resulting change in the peak acceleration is given in Figure 11. The amplitude of peak reduces significantly between 20 and 10 Hz hi-cut filter values. This can be interpreted as the significant contribution of the 8 Hz peak to the observed 0.8g peak in this component. The pedestal or the specific topographic features of the strong-motion site can play a role in this unusual peak. This will be investigated in the final version of this report.

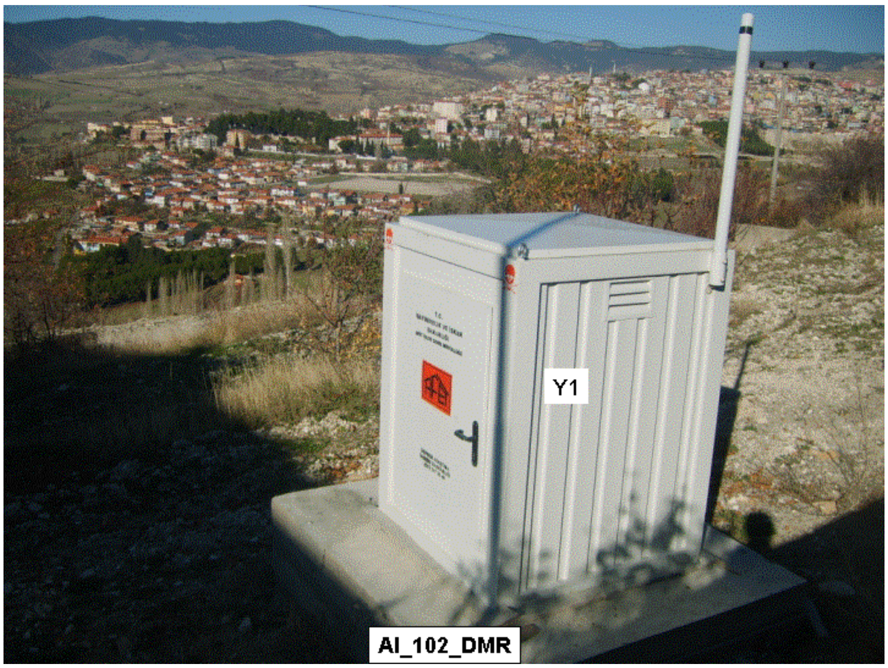

Figure 8. A view of the free field station of Demirci Station

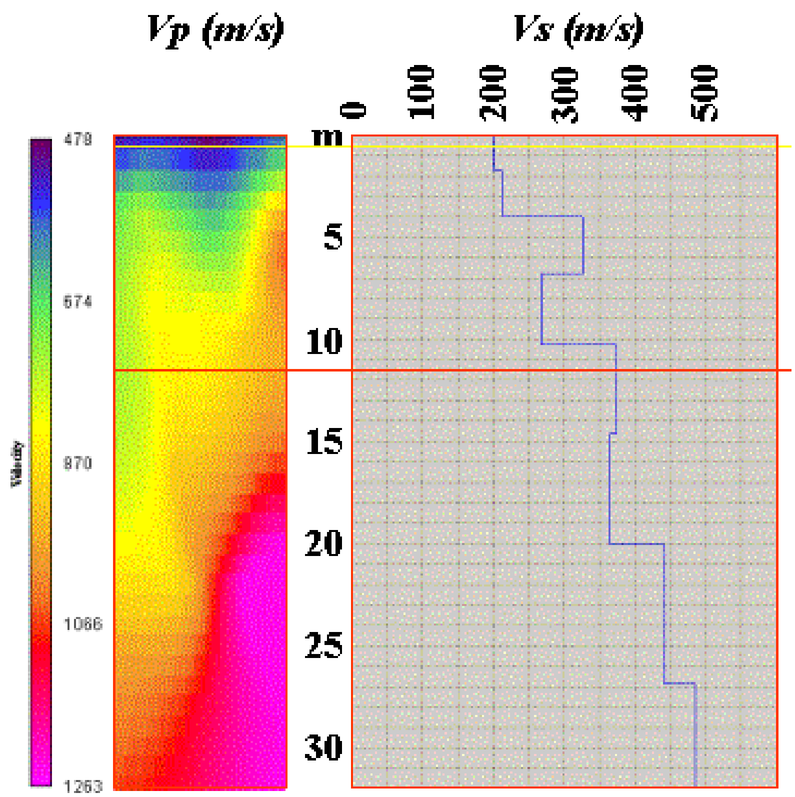

Figure 9. The P-wave velocity-depth model (left plot) and the S-wave velocity-depth profile (right plot) of the Demirci Station.

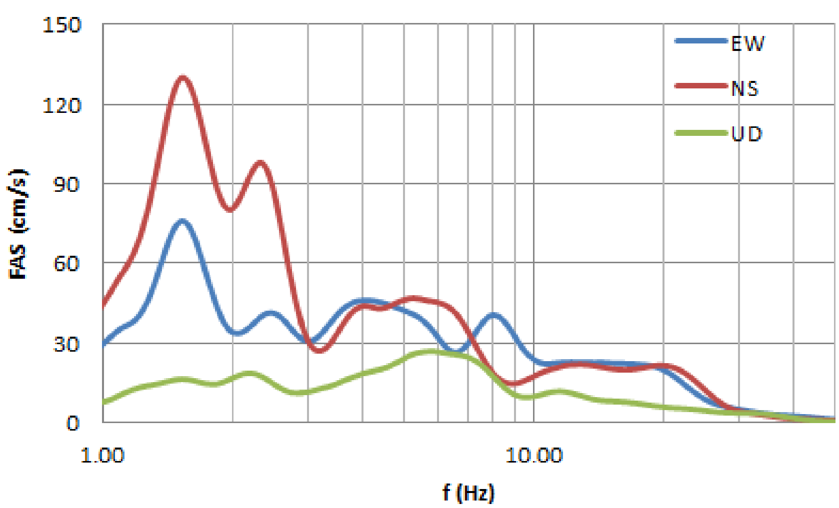

Figure 10. Smoothed Fourier acceleration spectra (FAS) of the EW, NS and UD components of the Demirci Recording

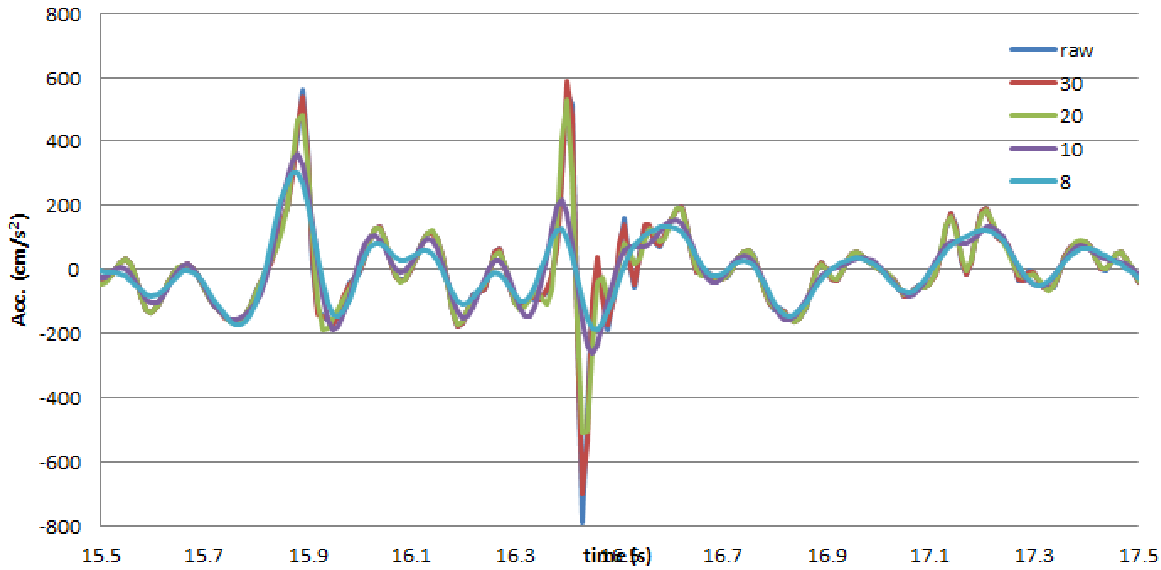

Figure 11. The acceleration time series of the EW component of the Demirci record for different hi-cut values

4. Observed damage on residential buildings

The Aegen region of Turkey, including Kütahya province is a highly active seismic area and has been exposed to earthquakes frequently. Kütahya is affected by the ground motions resulted from Gediz-Emet, Simav and Kütahya fault lines. In this region, the highest magnitude earthquake that could be measured was generated by Gediz fault on March 1970 and resulted in total collapse of 3500 buildings and more than 1000 casualties. The most recent ground shaking (Kütahya-Simav 2011 earthquake), approximately 40 km away from the epicenter of 1970 Gediz Earthquake, led to considerable damage in Simav, Kütahya (Figure 12). It should be noted that this earthquake was also originated by a normal fault as in 1970 Gediz Earthquake.

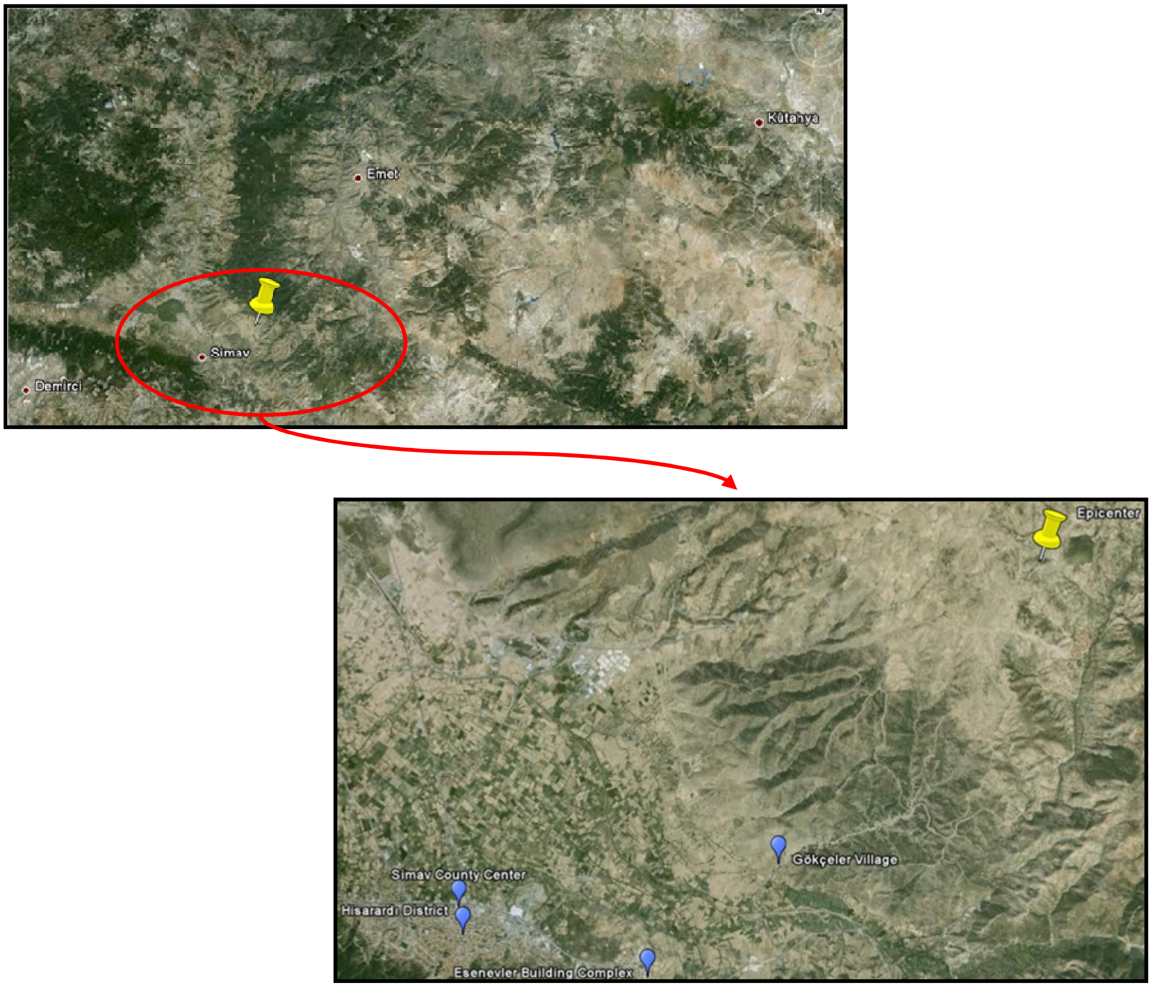

Figure 12. The epicenter of the Kütahya-Simav Earthquake and investigated sites

4.1. Observed structural damage

The post-earthquake observations pointed out that most severely affected sites in the region were Simav city center, Esenevler district, Gökçeler village and Hisarardı district (Figure 12). In this part of the report, the damage states of investigated buildings are discussed.

a) Simav County Center :

During the site investigations, the highest damage was observed in the vicinity of Simav city center which is 10 km away from the epicenter of earthquake. In Figure 13, the locations of buildings investigated in this site are shown on the map.

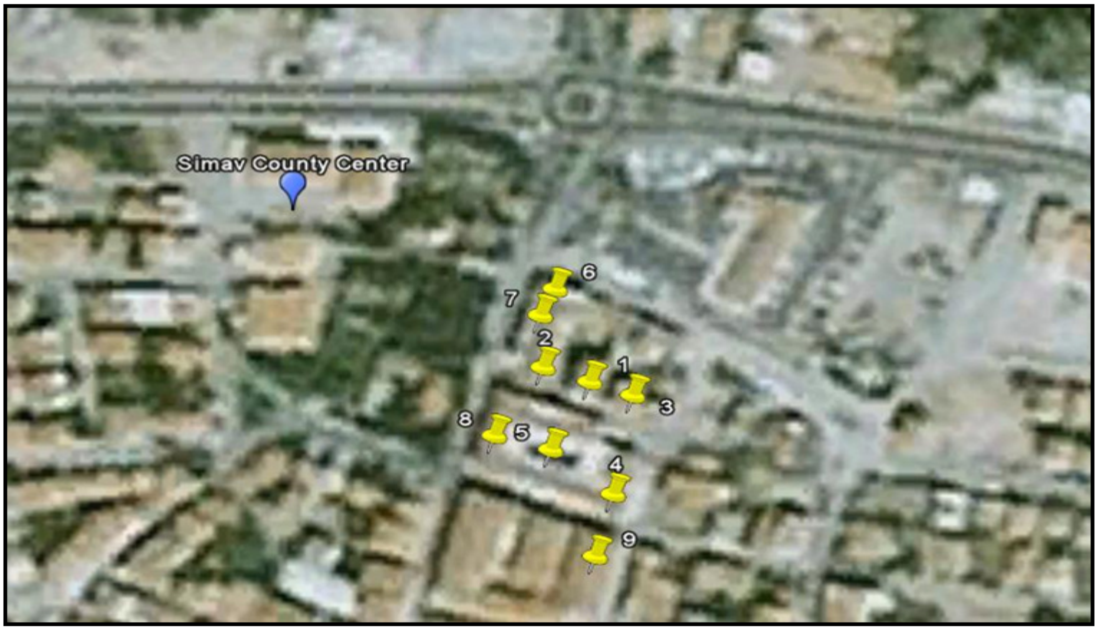

Figure 13. Map view of the buildings investigated in Simav county center

The site survey in Simav city center revealed that majority of the buildings had structural and/or non-structural damage. The main reasons of observed damage may be stated as structural system and member deficiencies, and fragility of the infill walls. Soft story formations and inadequate gap between buildings (i.e. to prevent pounding effect) are among the major structural deficiencies, as noticed by the first investigation of the damaged buildings from outside. The dense settlement in the city center and usage of the first stories as shops or stores (i.e. taller first stories and disuse of walls for exterior cladding) may be regarded as the reasons of these deficiencies. The soft stories caused by higher first floors and disuse of infill walls for exterior cladding may contribute to the extensive damage in the entrance level of these buildings. Such a building is presented in Figure 14. Although the building seemed to be undamaged from outside, wide shear cracks were observed on the first story columns, which had inadequate transverse reinforcement (Figure14.b and 14.c).

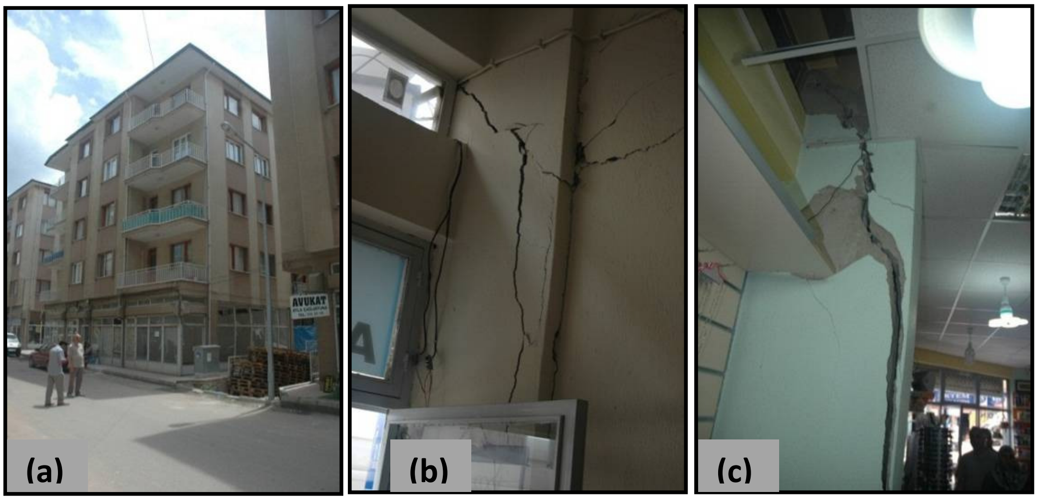

Figure 14. Soft story and resulting damages

During the survey of some buildings, the concrete compressive strength was measured by means of impact hammer testing in order to have an idea about the concrete quality. The coordinates of all investigated buildings were determined by a “GPS” device. Besides, a more detailed investigation was held for heavily damaged buildings by determining the structural plan and member details. The coordinates and damage state of the buildings investigated in the city center are presented in Table 4. Moreover, the outside view of the heavily damaged buildings are shown in Figure 15.

Figure 15. The outside view of the heavily damaged buildings in Simav county center: (a) - (b) Building 1; (c) Building 9

The details of observed damage of the investigated buildings in Simav city center can be explained on a building by building basis as follows:

i. Building 1:

This building was the only reinforced concrete structure that collapsed due to earthquake. The building had six stories and a basement (Figure 15.a- 4.b and Figure 15). The entrance story was a handmade carpet workshop and the remaining five stories used as residence before the earthquake.

The basement and last four stories of the building remained almost undamaged. Whereas, the first two stories were totally damaged, which resulted in leaning on the adjacent building after the earthquake. The building constructed adjacent to the collapsed building remained stable as shown in Figure 16. A close investigation of the building indicated that the strong axes of all columns were located in the long direction of the building. The measurements yielded concrete compressive strength of 10.8 MPa and 20 MPa for the beams and columns, respectively, in the second story. The building was observed to have serious errors in reinforcement detailing. The main deficiencies of the building may be listed as follows:

- Soft story,
- Inadequate gap between the neighbouring buildings-pounding effect,
- Poor concrete quality,
- Inadequate transverse reinforcement at beam-column joints,
- Excessive spacing of beam and column transverse reinforcement,
- Poor detailing of transverse reinforcement (i.e. with 90 degree hooks),
- Use of plain rebars for reinforcement,
- Weak column-strong beam (cross-sectional dimensions and reinforcement details of both beams and columns are provided in Figure 17).

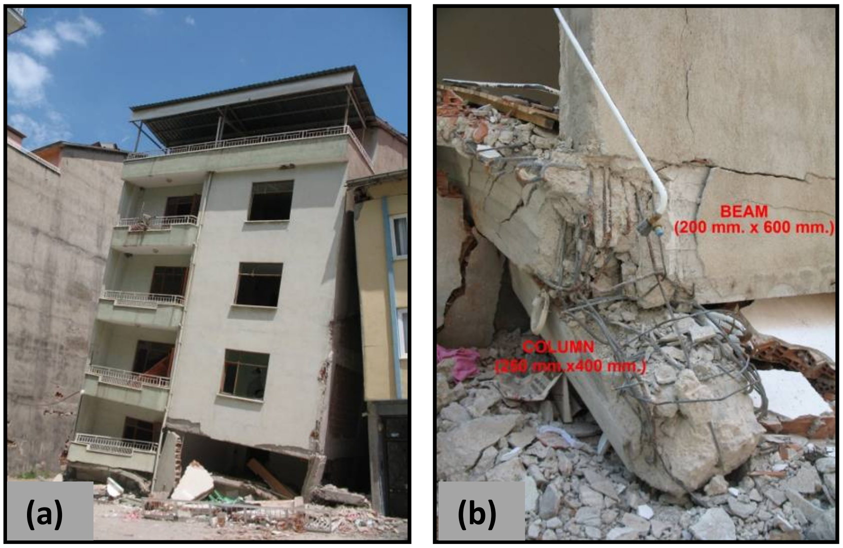

Figure 16. The collapsed building in Kütahya-Simav Earthquake (39.0920°N; 28.9793° E; 812 812 m)

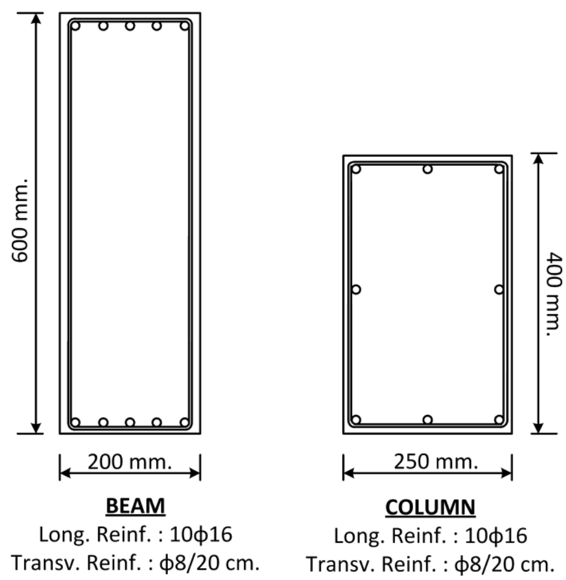

Figure 17. Cross-sectional dimensions and reinforcement details of beams and columns of the collapsed building

The most crucial structural system deficiency of “Building 1” was the arrangement of columns. As illustrated in Figure 18, the strong axes of all columns are in one direction only (i.e. parallel to each other). Therefore, the building did not have sufficient stiffness and strength to sustain the lateral earthquake demands in the short direction, resulting in total collapse. In order to mention the importance of this deficiency, the structural plan of another building (i.e. “Building 2”), which is located 10 m away from “Building 1” and had almost no structural damage due to earthquake, is presented in Figure 19. When structural plans of these two buildings are compared, it may be observed that “Building 2” has shear walls located in the short direction. The light damage experienced by “Building 2” with a minimum shear wall ratio indicates the significance of walls in providing structural safety.

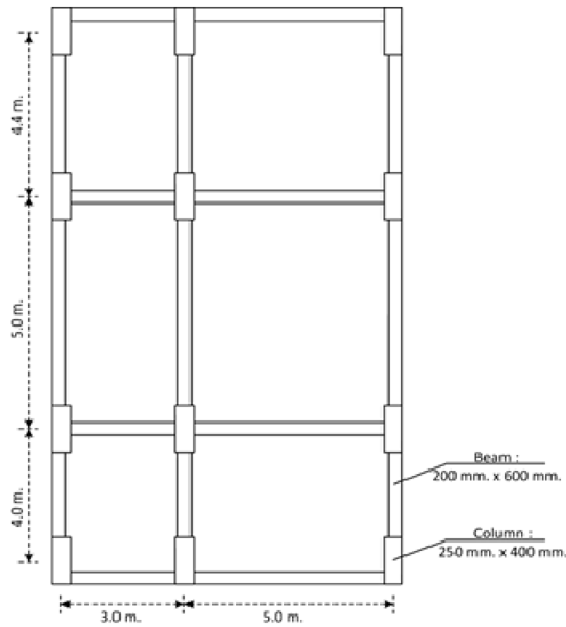

Figure 18. The Structural plan of “Building 1”

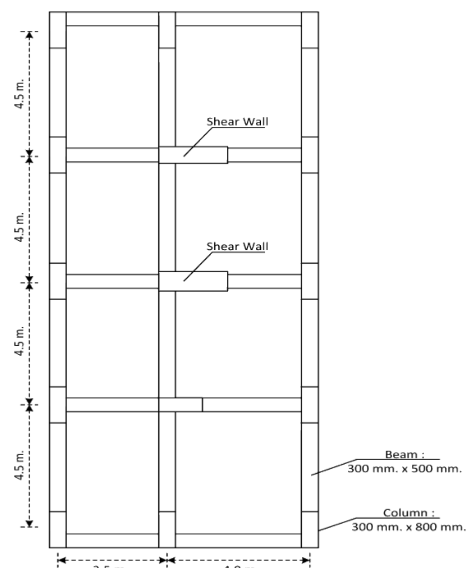

Figure 19. The Structural plan of “Building 2”

ii. Building 6:

“Building 6” is a two story building which had serious shear damage in almost all first story columns due to the earthquake. The wide shear cracks demonstrate the poor detailing and insufficient number of column transverse reinforcement (Figure 20). The observed damage in such a relatively low-rise building indicates how poor detailing may lead to catastrophic results.

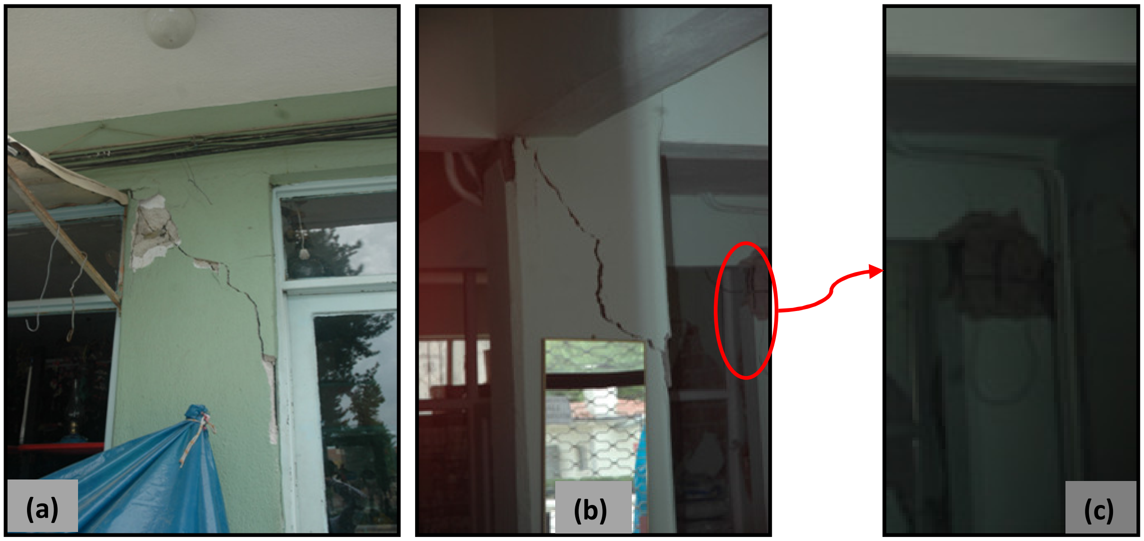

Figure 20. Damage of “Building 6”: (a) – (b) column shear cracks; (c) Plastic hinging at column ends

iii. Building 9:

“Building 9” which was constructed in 1998 is a five story residential building with shopping stores at the entrance level. The building was reported to be repaired after experiencing light damage in an earthquake occurred on 17th of February, 2009 (i.e. overcoating in one column and grouting for cracks). During the survey, the concrete compressive strength was measured as 15 MPa. Significant damage was observed on the first story columns due to recent Kütahya-Simav Earthquake (Figure 21). The major reason of shear damage on columns may be attributed to the poor detailing of transverse reinforcements.

Figure 21. Building 9 and the observed damage: (a) Outside view; (b) Column shear cracks; (c) Wide cracking at the upper ends of the columns

b) Hisarardı District:

Hisarardı district is located in Simav and is also approximately 10 km away from the epicenter of the earthquake. During the survey in Hisarardı, it was observed that majority of the investigated buildings experienced moderate damage. The types of observed damages were similar to those explained for Simav city center. On the other hand, heavy damage was observed in one of the buildings in the district. The map location and damage state of the building are given in Figure 22. The concrete compressive strength was measured as 20 MPa.

Figure 22. Building 10 and the observed damage: (a) Map view; (b) - (c) Insufficient gap between the buildings and wide shear cracks formed due to short column effect (39.0896°N; 28.9794°E; 818 m)

The adjacent construction of these buildings, where the required gap was not provided, prevented free movement of these structures and lead to pounding effect which further increased the damage. The adjacent buildings are shown in Figure 22.b. The higher building on the left caused significant damage on “Building 10” (i.e. having three stories on the right) due to pounding during the earthquake. The separation between two buildings and pounding damage on the shorter building may also be observed in Figure 22.b. Additionally, the windows at the top of first story infills resulted in a short column formation and corresponding wide shear cracks on the column (Figure 22.c). Besides, no other structural or member deficiency was observed in the building.

c) Gökçeler Village:

Gökçeler village is approximately 6 km away from the epicenter of the earthquake. After the first survey in the village, it was reported that 158 of 208 buildings in the village were damaged due to earthquake. The reason of this high damage ratio is the poor masonry construction of buildings in the village. The most significant damage was observed in some old and abandoned masonry buildings. The map locations of the buildings which experienced moderate or heavy damage are presented in Figure 23. The GPS coordinates and damage state of these buildings are also provided in Table 5.

Figure 23. The map view of the buildings in Gökçeler village

i. Building 11:

The damage on the reinforced concrete building, Building 11, which has three stories are shown in Figure 24. It was observed that the lateral reinforcement spacing at the column ends were insufficient and the free ends of ties were bent 90^0 instead of 135^0 (Figure 24.b). Besides, after crushing of the infill walls at the corners, the columns were subjected to high shear demands at these regions due to formation of a short column (Figure 24.c). When it was considered that the building was constructed in a village with limited engineering design and control service, it should be considered as a lucky survivor since such deficiencies did not result in the collapse of the building.

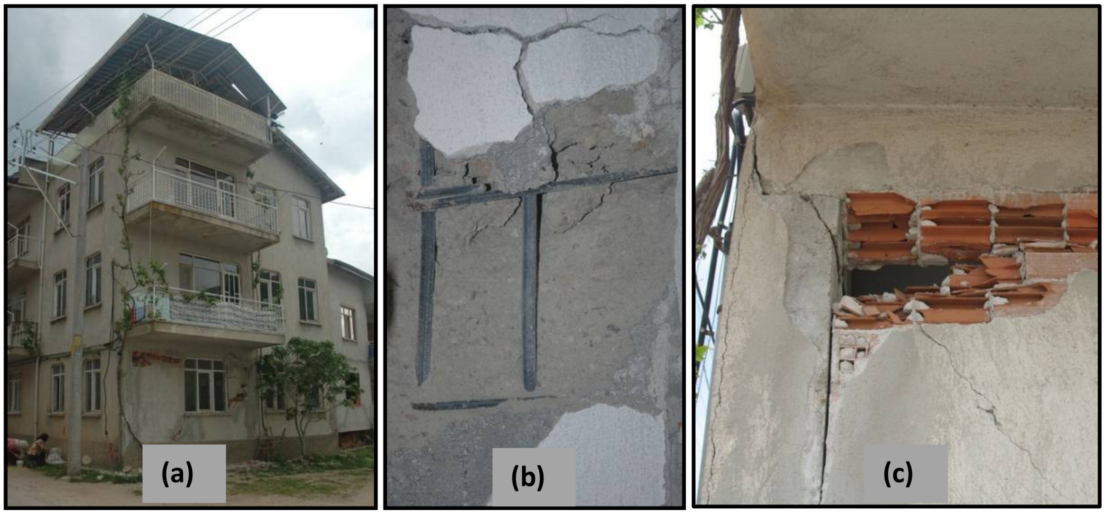

Figure 24. Three-story building in Gökçeler village and observed damage (Building 11)

ii. Gökçeler Mosque:

The mosque of Gökçeler village was constructed in 1998 (Figure 25). The earthquake performance of the main structure may be regarded as successful since the structure did not experience significant damage. However, earthquake damage to mosques generally indicate that minarets may sustain much severe damage then the main structure as was the case in Gökçeler, Figure 25. The performance and earthquake stability of the masonry type minaret should be investigated more thoroughly considering the actual material strength and imposed demand on this distributed mass structure.

Figure 25. Damage of the mosque in Gökçeler village

d) Esenevler Building Complex:

Four buildings were investigated in Esenevler building complex, which is approximately 8 km from the epicenter of the earthquake. The map locations of these buildings are shown in

Figure 26. The GPS coordinates and damage states of the same buildings are also given in Table 6.

The eight-story reinforced concrete buildings of the complex, which were constructed between 1995-99, are considerably less damaged compared to the other buildings in other districts of Simav. During the survey, it was deduced that the code regulations were mostly applied during the design and construction stages of the buildings. All buildings had shear walls as lateral load carrying systems which has cross-sectional dimensions of 250 mm x 1250 mm. The occupants who were present during the construction of buildings indicated that the lateral reinforcement spacing was decreased at both column critical ends (i.e. having a spacing of 100 mm). It was also stated that ties were provided at the beam-column joints. The major observable deficiency of the buildings was the use of plain rebars for both longitudinal and transverse reinforcement. Another observation was that poor plaster and infill wall quality. This may be observed as fallen-off plasters in large areas (Figure 27.c). These non-structural damages not only caused a psychological effect on the occupants but also resulted in incursion in their living spaces. Therefore, some of the occupants did not want to go into the buildings even there were no structural damage.

Figure 26. The map view of buildings in Esenevler building complex

i. A-Block:

A-Block of Esenevler building complex has eight stories over a basement, the same as the other buildings in the complex. It was stated that the plaster fell off partially in some regions of the building during the earthquake that occurred two years ago and re-plastered afterwards. Besides, it was also mentioned that the building was affected by 1999 Izmit

Earthquake when it was at the construction state in that time. During the survey, it was observed that the building had infill wall damage and hairline beam cracks only in the first four stories.

ii. B-Block:

In the investigation of B-Block, crushing of cover concrete was observed at some stair joints. There were no other damage indications, except infill wall damage and hairline beam cracks in the first stories.

iii. C-Block:

The concrete compressive strength was determined as approximately 20 MPa. In the building, infill wall damage and hairline flexural cracks were observed on some beams in the first four stories (Figures 27.b and c). The width of these cracks support the fact that the damage can be classified as light to moderate.

Figure 27. (a) C-Block of Esenevler building complex and (b) - (c) Damage state

iv. Sayar and Peker Apartment:

Among all the other investigated buildings in Esenevler, Sayar and Peker Apartment (Figure 28.a) had the highest damage. The building was constructed after 1999 Izmit Earthquake. The diagonal cracks, local crushing and spillage of the plaster was observed on the infill walls, as in other buildings in Esenevler (Figure 28.b). Besides, the beam and column cover concrete crushed in some certain locations on the building facade (Figure 28.c).

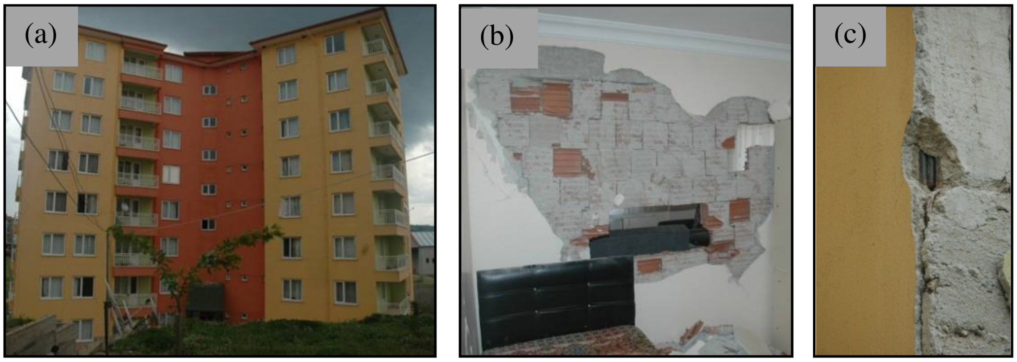

Figure 28. (a) Esenevler building complex, Sayar and Peker apartment, (b) Infill wall damage and (c) Crushing of cover concrete

4.2. Summary and conclusive observations

Site investigations after Kütahya-Simav Earthquake point out that this moderate earthquake event caused serious damage to a significant number of buildings and the financial loss is expected to be a large portion of the regional economy. In general, the structures seem undamaged from outside but partition wall and even column damages are encountered after the interior investigations are completed.

The most remarkable construction error in Simav is the inadequate gap between the neighboring buildings. In Simav city center, nearly all of the buildings are placed adjacent to another without sufficient space for building deformations.

The other interesting observation is that nearly all of the buildings lack proper reinforcement detailing especially for the confining and transverse reinforcement. For instance, shear cracks were observed in many frame buildings. These shear cracks are surely due to the large spacing of stirrups and improper end zone confinement of both column and beam.

Additionally, the use of plain bars and low quality concrete were the most noticeable deficiency observed in damaged structures. This is similar to previous observations in other regions of Turkey. Use of low strength concrete causes adherence problems in reinforced concrete members, which in turn results in significant plastic hinge damage (See Figure 29). Another significant detailing problem is the use of insufficient lap splice length for the longitudinal reinforcement. Nearly, all of the investigated buildings reveal that the longitudinal reinforcements are lapped at the base of columns (Figure 29.b) over an insufficient length.

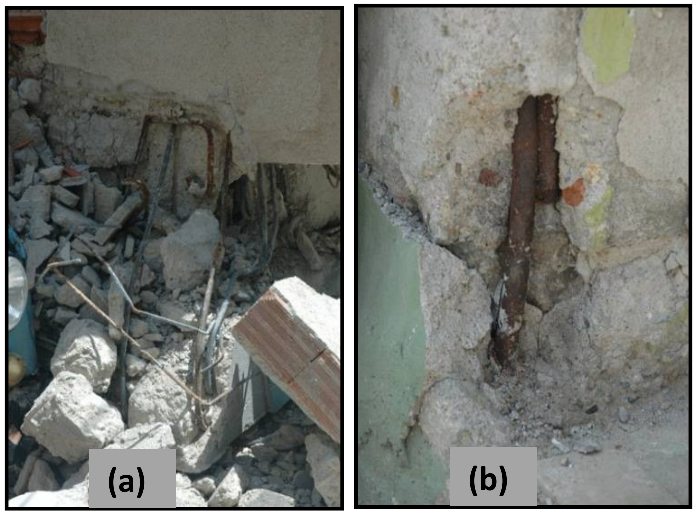

Figure 29. Adherence problems due to plain bars

Figure 30. (a) Lack of stirrups at the joints and (b) Redundancy of columns (Building 5)

Another problem observed in Simav is the lack of stirrups at the joints. This detailing mistake makes the column-beam joints vulnerable to earthquake induced effects and heavy damage is inevitable at those regions. This situation is illustrated in Figure 30. The three adjacent frame buildings (Building 5) are well – separated from each other (no pounding effect) in this case. In addition to improper detailing of the reinforcement, these buildings have weak and soft storey irregularities. However, the redundancy of columns provided the safety of these buildings (See Figure 30.b).

The structural damage observed in Simav is in parallel to the earthquake damage observed in site investigations of previous earthquakes in Turkey. Especially, weak and soft storey problems, improper reinforcement detailing of columns and joints and pounding and insufficient anchorage of infill walls are the main reasons of observed damage. The insufficient spacing of buildings, particularly seen in Central and Western Anatolia, causes the increase in the expected damage. As a result of the field inspections, the followings are suggested to be utilized in research and development studies.

1. Partition walls should be built with precautions against out of plane collapse and spalling of heavy plaster layers. This may prevent the heavy financial and most importantly life losses.
2. Keeping in mind that the currently applied techniques fail to assess even a relatively small building stock for tagging. This could be quite troublesome for large scale disasters. Hence, site investigation methods to determine building damage level and to decide whether to allow building use or not for moderate damage levels are needed. In this way, the population affected by the earthquake could return their normal life easily.

It is thought that the observed detailing mistakes are stemmed from illiteracy rather than intention. Therefore, local contractors and designers, particularly in small cities and counties, should be educated on earthquake resistant design at a nationwide scale.

References:

Abrahamson, N.A. and Silva, W.J. (1997). Empirical response spectral attenuation relations for shallow crustal earthquakes, *Seismological Research Letters*, 68: 94-127.

Abrahamson, N.A. and Silva, W. (2008). Summary of the Abrahamson and Silva NGA ground motion relations, *Earthquake Spectra*, 24: 67-98.

Akkar, S. and Bommer, J.J., (2006). " Influence of long-period filter cut-off on elastic spectral displacements," *Earthquake Engineering and Structural Dynamics* , 35(9), 1145-1165.

Akkar, S. and Bommer, J.J.,(2010). Empirical Equations for the Prediction of PGA, PGV and Spectral Accelerations in Europe, the Mediterranean Region and the Middle East, *Manuscript accepted for publication in Seismological Research Letters,* Vol:81, 195-206.

Akkar S. and Cagnan Z. (2010). A local ground motion predictive model for Turkey and its comparison with other regional and global ground-motion models, submitted to Bull. Seism. Soc. Am. for publication.

Akkar, S., Kale, O., Yenier, E. and Bommer J.J., 2011. The high-frequency limit of usable response spectral ordinates from filtered analogue and digital strong-motion accelerograms, Earthquake Engineering and Structural Dynamics, DOI: 10.1002/eqe.1095

Boore, D. M. and Atkinson, G. M. (2008). Ground motion prediction equations for the average horizontal component of PGA, PGV, and 5%-damped PSA at spectral periods between 0.01 s and 10.0 s, *Earthquake Spectra*, Vol. 24, No. 1, pp. 99-138.

Boore, D. M., and G. M. Atkinson (2008). Ground motion prediction equations for the average horizontal component of PGA, PGV, and 5%-damped PSA at spectral periods between 0.01 s and 10.0 s. *Earthquake Spectra* 24 (1), 99–138.

Campbell, K. W., and Y. Bozorgnia (2008). NGA ground motion model for the geometric mean horizontal component of PGA, PGV, PGD and 5% damped linear elastic response spectra for periods ranging from 0.01 to 10 s. *Earthquake Spectra* 24 (1), 139–172.

Chiou, B. S.-J, and R. R. Youngs (2008). An NGA model for the average horizontal component of peak ground motion and response spectra. *Earthquake Spectra* 24 (1), 173–215.

Douglas, J., (2003). What is a poor quality strong-motion record?, *Bulletin of Earthquake Engineering*, 1: 141-156.

Douglas, J. and D. M. Boore (2011). High-frequency filtering of strong-motion records, *Bull. Earthquake Engineering,* 9 ,395--409. (862 Kb).

Kaklamanos, et al (2011). Estimating unknown input parameters when implementing the NGA ground-motion prediction equations in engineering practice. *Earthquake Spectra*.
Koçyiğit, 2011.written communication

Table 1. Important seismological features of the earthquake reported by national and international seismological agencies

Agency	Date	Time (GMT)	Epicenter Latitude	Epicenter Longitude	Depth (km)	M_w	M_b	M_s	M_L	M_0 (dyne.cm)
DEMP[2]	19/05/2011	20:15:22.79	39.1328	29.0820	24.46	5.8	-	-	5.7	3.98e+17-
KOERI[3]	19/05/2011	23:15:23	39.152	29.088	7.6	-	-	-	5.9	-
GCMT	19/05/2011	20:15:28.4	39.14	29.08	12	5.9	6.0	6.0	-	8.63e+17
USGS1	19/05/2011	20:15:24.42	39.104	29.099	11	5.8	-	-	-	6.8e+17
USGS2	19/05/2011	20:15:23	39.114	29.124	15	5.8	-	-	-	6.7e+17

Agency	T-axes PLG	T-axes AZ	N-axes PLG	N-axes AZ	P-axes PLG	P-axes AZ	1st Plane Strike	1st Plane Dip	1st Plane Slip	2nd Plane Strike	2nd Plane Dip	2nd Plane Slip	Correct Plane
DEMP	-	-	-	-	-	-	315	56	-79				
KOERI	-	-	-	-	-	-	-	-	-	-	-	-	-
GCMT	-	-	-	-	-	-	275	45	-102	111	46	-78	2
USGS1	7	14	27	280	62	118	131	44	-50	262	58	-122	1
USGS2	8	194	7	285	78	55	275	37	-102	111	54	-80	2

[2] Earthquake Department of the Disaster and Emergency Management Presidency.
[3] Kandilli Observatory and Earthquake Research Institute

Table 2. Important properties of the processed records from the event

Record Names	Instrument Type	Record Information	f_{lc}-NS	f_{hc}-NS	Usable period-NS	f_{lc}-EW	f_{hc}-EW	Usable period-EW	f_{lc}-UD	f_{hc}-UD	Usable period-UD
20110519201522_0302	Guralp cmg5td		0.05	30	19.4	0.05	30	19.4	0.05	30	19.4
20110519201522_0905	Guralp cmg5td		0.05	10	18.0	0.05	30	18.0	0.05	25	18.0
20110519201522_0910	Guralp cmg5td		0.10	20	8.0	0.05	20	16.0	0.05	0	16.0
20110519201522_1006	Guralp cmg5td	ms	0.05	40	19.4	0.05	30	19.4	0.05	0	19.4
20110519201522_1009	Guralp cmg5td	ms	0.07	30	12.9	0.05	0	18.0	0.05	30	18.0
20110519201522_1014	Guralp cmg5td	ms	0.05	20	18.0	0.07	30	12.9	0.05	0	18.0
20110519201522_1102	Guralp cmg5td		0.05	35	18.0	0.05	25	18.0	0.05	0	18.0
20110519201522_1601	Kinemetrics etna		0.05	30	19.4	0.10	20	9.7	0.05	40	19.4
20110519201522_1607	Kinemetrics etna	ms	0.10	20	8.0	0.05	20	16.0	0.05	40	16.0
20110519201522_1608	Kinemetrics etna		0.05	15	18.0	0.05	15	18.0	0.05	0	18.0
20110519201522_1609	Kinemetrics etna	ms	0.15	20	6.5	0.07	25	13.9	0.05	0	19.4
20110519201522_1613	Guralp cmg5td	ms	0.05	0	18.0	0.10	0	9.0	0.05	30	18.0
20110519201522_1614	Guralp cmg5td	ms	0.07	25	13.9	0.05	25	19.4	0.05	0	19.4
20110519201522_1615	Kinemetrics etna		0.07	30	13.9	0.05	30	19.4	0.05	0	19.4
20110519201522_1616	Kinemetrics etna		0.05	30	18.0	0.07	30	12.9	0.05	30	18.0
20110519201522_1617	Kinemetrics etna		0.05	0	16.0	0.05	0	16.0	0.05	0	16.0
20110519201522_1618	Guralp cmg5td	ms	0.05	25	16.0	0.05	35	16.0	0.05	40	16.0
20110519201522_2008	Guralp cmg5td		0.10	10	8.0	0.05	10	16.0	0.05	10	16.0
20110519201522_2009	Guralp cmg5td		0.05	30	16.0	0.05	30	16.0	0.05	35	16.0
20110519201522_2011	Guralp cmg5td		0.07	15	11.4	0.05	20	16.0	0.05	20	16.0
20110519201522_2601	Guralp cmg5td		0.07	25	13.9	0.10	20	9.7	0.07	20	13.9
20110519201522_2602	Guralp cmg5td		0.05	0	19.4	0.07	25	13.9	0.05	0	19.4
20110519201522_2603	Guralp cmg5td	spike, ms	0.05	40	18.0	0.05	35	18.0	0.05	40	18.0

Record Names	Instrument Type	Record Information	f_{lc}-NS	f_{hc}-NS	Usable period-NS	f_{lc}-EW	f_{hc}-EW	Usable period-EW	f_{lc}-UD	f_{hc}-UD	Usable period-UD
20110519201522_2604	Guralp cmg5td	ms	0.05	25	19.4	0.10	25	9.7	0.05	25	19.4
20110519201522_2605	Guralp cmg5td	ms	0.05	20	16.0	0.05	30	16.0	0.05	35	16.0
20110519201522_2607	Guralp cmg5td		0.05	30	19.4	0.07	25	13.9	0.07	0	13.9
20110519201522_2608	Guralp cmg5td		0.05	0	18.0	0.05	0	18.0	0.05	40	18.0
20110519201522_2610	Guralp cmg5td	ms	0.05	0	16.0	0.05	0	16.0	0.05	0	16.0
20110519201522_2611	Guralp cmg5td	ms	0.07	0	11.4	0.05	0	16.0	0.07	0	11.4
20110519201522_2613	Guralp cmg5td	ms	0.05	25	16.0	0.10	25	8.0	0.05	35	16.0
20110519201522_2614	Guralp cmg5td		0.05	30	16.0	0.10	25	8.0	0.07	15	11.4
20110519201522_2615	Guralp cmg5td	ms	0.05	25	16.0	0.05	25	16.0	0.05	25	16.0
20110519201522_2616	Guralp cmg5td	ms	0.05	25	16.0	0.05	20	16.0	0.05	25	16.0
20110519201522_3202	Guralp cmg5td	Not filtered									
20110519201522_3405	Guralp cmg5td		0.05	20	16.0	0.05	25	16.0	0.05	20	16.0
20110519201522_3406	Guralp cmg5td		0.05	35	16.0	0.05	25	16.0	0.05	20	16.0
20110519201522_3409	Guralp cmg5td	ms	0.05	25	16.0	0.05	20	16.0	0.05	30	16.0
20110519201522_3410	Guralp cmg5td		0.05	25	16.0	0.10	30	8.0	0.05	0	16.0
20110519201522_3503	Guralp cmg5td		0.05	30	19.4	0.07	40	13.9	0.07	40	13.9
20110519201522_3506	Guralp cmg5td	ms	0.05	20	16.0	0.05	20	16.0	0.05	30	16.0
20110519201522_3510	Guralp cmg5td	ms	0.05	20	16.0	0.05	20	16.0	0.07	30	11.4
20110519201522_3511	Guralp cmg5td	ms	0.05	35	16.0	0.05	35	16.0	0.05	35	16.0
20110519201522_3512	Guralp cmg5td	ms	0.05	12	16.0	0.05	25	16.0	0.05	0	16.0
20110519201522_3514	Guralp cmg5td		0.05	20	16.0	0.05	20	16.0	0.07	25	11.4
20110519201522_3515	Guralp cmg5td	ms	0.05	20	16.0	0.05	20	16.0	0.07	30	11.4
20110519201522_3517	Guralp cmg5td		0.05	20	16.0	0.05	25	16.0	0.05	25	16.0
20110519201522_2604	Guralp cmg5td	ms	0.05	25	19.4	0.10	25	9.7	0.05	25	19.4
20110519201522_2605	Guralp cmg5td	ms	0.05	20	16.0	0.05	30	16.0	0.05	35	16.0
20110519201522_2607	Guralp cmg5td		0.05	30	19.4	0.07	25	13.9	0.07	0	13.9
20110519201522_2608	Guralp cmg5td		0.05	0	18.0	0.05	0	18.0	0.05	40	18.0
20110519201522_2610	Guralp cmg5td	ms	0.05	0	16.0	0.05	0	16.0	0.05	0	16.0

Record Names	Instrument Type	Record Information	f_{lc}-NS	f_{hc}-NS	Usable period-NS	f_{lc}-EW	f_{hc}-EW	Usable period-EW	f_{lc}-UD	f_{hc}-UD	Usable period-UD
20110519201522_3518	Guralp cmg5td	ms	0.05	0	16.0	0.05	0	16.0	0.07	30	11.4
20110519201522_3519	Guralp cmg5td		0.05	20	16.0	0.07	0	11.4	0.05	0	16.0
20110519201522_3520	Guralp cmg5td		0.05	25	16.0	0.05	25	16.0	0.05	30	16.0
20110519201522_3521	Guralp cmg5td	ms	0.15	15	5.3	0.07	15	11.4	0.05	30	16.0
20110519201522_3522	Guralp cmg5td	ms	0.15	25	5.3	0.05	12	16.0	0.05	30	16.0
20110519201522_3524	Guralp cmg5td	ms	0.05	30	16.0	0.07	20	11.4	0.05	35	16.0
20110519201522_3525	Guralp cmg5td		0.05	25	16.0	0.05	25	16.0	0.07	30	11.4
20110519201522_3530	Guralp cmg5td		0.05	25	16.0	0.05	25	16.0	0.05	30	16.0
20110519201522_4102	Guralp cmg5td	ms	0.10	15	8.0	0.10	15	8.0	0.07	15	11.4
20110519201522_4103	Guralp cmg5td	Not filtered									
20110519201522_4104	Guralp cmg5td	ms	0.05	25	16.0	0.10	30	8.0	0.05	0	16.0
20110519201522_4105	Guralp cmg5td	ms	0.05	30	19.4	0.05	30	19.4	0.05	0	19.4
20110519201522_4106	Guralp cmg5td	ms	0.05	25	18.0	0.07	30	12.9	0.05	35	18.0
20110519201522_4107	Guralp cmg5td	ms	0.05	15	16.0	0.07	20	11.4	0.05	25	16.0
20110519201522_4108	Guralp cmg5td	ms	0.07	20	11.4	0.07	20	11.4	0.05	15	16.0
20110519201522_4110	Guralp cmg5td	ms	0.05	20	16.0	0.07	20	11.4	0.05	20	16.0
20110519201522_4111	Guralp cmg5td	ms	0.05	25	16.0	0.05	25	16.0	0.05	30	16.0
20110519201522_4113	Guralp cmg5td	ms	0.05	40	16.0	0.07	40	11.4	0.05	40	16.0
20110519201522_4115	Guralp cmg5td	ms	0.07	20	11.4	0.07	15	11.4	0.05	30	16.0
20110519201522_4116	Guralp cmg5td	ms	0.05	20	16.0	0.10	20	8.0	0.05	20	16.0
20110519201522_4301	Guralp cmg5td		0.05	40	19.4	0.07	40	13.9	0.05	40	19.4
20110519201522_4304	Güralp cmg5td	ms	0.10	40	9.7	0.05	40	19.4	0.07	25	13.9
20110519201522_4305	Guralp cmg5td	Not filtered									
20110519201522_3518	Guralp cmg5td	ms	0.05	0	16.0	0.05	0	16.0	0.07	30	11.4
20110519201522_3519	Guralp cmg5td		0.05	20	16.0	0.07	0	11.4	0.05	0	16.0
20110519201522_3520	Guralp cmg5td		0.05	25	16.0	0.05	25	16.0	0.05	30	16.0
20110519201522_3521	Guralp cmg5td	ms	0.15	15	5.3	0.07	15	11.4	0.05	30	16.0
20110519201522_3522	Guralp cmg5td	ms	0.15	25	5.3	0.05	12	16.0	0.05	30	16.0

Record Names	Instrument Type	Record Information	f_{lc}-NS	f_{hc}-NS	Usable period-NS	f_{lc}-EW	f_{hc}-EW	Usable period-EW	f_{lc}-UD	f_{hc}-UD	Usable period-UD
20110519201522_4306	Guralp cmg5td	ms	0.07	30	11.4	0.05	30	16.0	0.05	25	16.0
20110519201522_4501	Guralp cmg5td		0.05	25	19.4	0.05	20	19.4	0.05	30	19.4
20110519201522_4502	Guralp cmg5td		0.07	0	13.9	0.07	0	13.9	0.05	0	19.4
20110519201522_4504	Guralp cmg5td	ms	0.10	40	9.7	0.10	10	13.9	0.10	40	9.7
20110519201522_4506	Guralp cmg5td		0.05	35	19.4	0.07	35	13.9	0.05	0	19.4
20110519201522_5905	Guralp cmg5td		0.05	20	16.0	0.05	20	16.0	0.05	25	16.0
20110519201522_6401	Güralp cmg5td		0.05	20	19.4	0.05	20	19.4	0.05	20	19.4
20110519201522_7701	Kinemetrics etna		0.30	18	3.0	0.30	30	3.0	0.40	0	2.3
20110519201522_7702	Kinemetrics etna		0.05	25	19.4	0.05	40	19.4	0.05	30	19.4
20110519201522_8103	Guralp cmg5td	ms	0.05	20	16.0	0.05	20	16.0	0.05	30	16.0
20110519201522_8104	Guralp cmg5td		0.05	10	16.0	0.10	10	8.0	0.05	25	16.0
20110519201522_8105	Guralp cmg5td		0.05	15	16.0	0.07	30	11.4	0.05	15	16.0
20110519201522_8107	Guralp cmg5td		0.05	15	16.0	0.05	15	16.0	0.05	10	16.0
20110519201522_8108	Guralp cmg5td		0.05	10	16.0	0.10	15	8.0	0.05	20	16.0
20110519201558_3523	Guralp cmg5td		0.05	15	16.0	0.05	15	16.0	0.07	15	11.4

f_{lc}: Low-cut filter frequency
f_{hc}: High-cut filter frequency
ms: multi-shock event
Not filtered: The data is not filtered since the waveform quality is low.

Table 2 (continued)

Record Names	Processed PGA_EW (cm/s^2)	Processed PGA_NS (cm/s^2)	Processed PGA_UD (cm/s^2)	Processed PGV_EW (cm/s)	Processed PGV_NS (cm/s)	Processed PGV_UD (cm/s)
20110519201522_0302	10.658	6.7741	3.6966	2.0695	1.2015	0.58845
20110519201522_0905	1.5007	1.3266	1.0424	0.42678	0.17894	0.1671
20110519201522_0910	2.3851	3.1462	2.7226	0.76995	0.87938	0.54723
20110519201522_1006	18.311	15.99	8.6354	1.9119	1.5615	0.74284
20110519201522_1009	16.713	16.322	10.187	1.3515	0.9107	0.81388
20110519201522_1014	5.0412	4.5136	2.3859	0.54421	0.44852	0.22166
20110519201522_1102	14.658	11.586	5.7252	0.98006	0.89919	0.40158
20110519201522_1601	12.895	1.4118	4.8217	1.6644	0.075163	1.0652
20110519201522_1607	18.515	19.813	9.0778	3.3786	4.3552	1.2515
20110519201522_1608	11.339	7.864	3.868	0.76908	1.5473	0.49983
20110519201522_1609	19.24	19.626	9.6707	1.6087	2.3938	0.92662
20110519201522_1613	24.623	17.242	9.099	1.7256	1.2442	0.75699
20110519201522_1614	29.362	62.231	16.738	2.3519	3.5973	0.88019
20110519201522_1615	9.1141	14.596	5.1937	1.2255	2.704	0.67345
20110519201522_1616	4.6766	3.0621	1.9502	0.46797	0.45705	0.42226
20110519201522_1617	7.7073	9.9907	4.0376	0.39914	0.61267	0.43798
20110519201522_1618	13.636	15.122	5.939	1.0682	0.83401	0.29273
20110519201522_2008	2.773	3.3314	1.9805	0.39914	0.44969	0.30766
20110519201522_2009	9.3554	7.6137	4.1113	1.9216	1.224	0.70213
20110519201522_2011	1.1464	0.80516	0.81672	0.26328	0.22252	0.24414
20110519201522_2601	6.9839	6.7008	3.4131	0.62725	0.45385	0.27189
20110519201522_2602	5.851	8.4098	3.4295	0.74055	1.1555	0.58953
20110519201522_2603	5.089	9.6648	4.0622	0.52955	0.69274	0.35483
20110519201522_2604	8.8806	11.053	3.3482	0.88669	1.085	0.34094
20110519201522_2605	12.232	14.444	4.0349	0.9858	0.84847	0.60191
20110519201522_2607	6.3487	8.3708	5.485	0.79475	0.98921	0.74833
20110519201522_2608	1.6377	1.4765	1.2281	0.17829	0.16332	0.19267

Record Names	Processed PGA_EW (cm/s^2)	Processed PGA_NS (cm/s^2)	Processed PGA_UD (cm/s^2)	Processed PGV_EW (cm/s)	Processed PGV_NS (cm/s)	Processed PGV_UD (cm/s)
20110519201522_2610	11.74	10.635	5.0285	1.5025	1.5018	0.45653
20110519201522_2611	10.696	9.9004	4.6151	1.2995	1.3325	0.77606
20110519201522_2613	11.632	8.3993	4.1168	1.2042	1.084	0.39462
20110519201522_2614	3.9996	4.5009	2.1376	0.58308	0.58108	0.34567
20110519201522_2615	6.4472	9.8677	4.7093	1.3253	1.3228	0.55401
20110519201522_2616	5.5235	4.2211	2.6523	0.50472	0.49424	0.31042
20110519201522_3202						
20110519201522_3405	1.7097	1.2975	0.89693	0.14178	0.12005	0.16072
20110519201522_3406	2.4647	3.1794	2.0313	0.14723	0.18629	0.18767
20110519201522_3409	5.7492	6.0961	2.4895	0.51726	0.35009	0.25069
20110519201522_3410	4.6829	4.0057	1.4339	0.32752	0.32018	0.24623
20110519201522_3503	6.1692	7.5715	1.9186	0.91694	0.6602	0.22011
20110519201522_3506	2.0813	2.9227	1.0513	0.266	0.2756	0.13168
20110519201522_3510	4.2278	4.5399	1.1931	0.41452	0.35671	0.19302
20110519201522_3511	2.4426	2.2953	1.0789	0.34113	0.25386	0.17006
20110519201522_3512	2.7819	2.8632	0.99311	0.37142	0.21616	0.15848
20110519201522_3514	3.7186	2.6228	1.8474	0.47214	0.34919	0.18953
20110519201522_3515	7.2461	5.7938	3.692	0.99215	0.78651	0.41621
20110519201522_3517	2.5424	1.6691	1.3207	0.33091	0.25907	0.25631
20110519201522_3518	7.6736	9.0274	4.0258	0.95134	1.0007	0.52422
20110519201522_3519	6.5355	7.6674	3.0615	1.4033	1.181	0.53231
20110519201522_3520	2.9498	2.8619	3.3851	0.42425	0.32656	0.4743
20110519201522_3521	8.8845	8.0372	2.422	1.5945	1.159	0.46166
20110519201522_3522	5.5312	5.531	2.6285	0.8038	0.76298	0.34172
20110519201522_3524	2.8157	2.7722	1.4081	0.30821	0.23903	0.14787
20110519201522_3525	3.1177	2.3959	1.2064	0.40539	0.19989	0.16304
20110519201522_3530	6.339	8.9207	2.97	0.85592	0.88838	0.23634
20110519201522_2610	11.74	10.635	5.0285	1.5025	1.5018	0.45653

Record Names	Processed PGA_EW (cm/s^2)	Processed PGA_NS (cm/s^2)	Processed PGA_UD (cm/s^2)	Processed PGV_EW (cm/s)	Processed PGV_NS (cm/s)	Processed PGV_UD (cm/s)
20110519201522_4102	1.5136	1.389	0.6461	0.20995	0.2368	0.23376
20110519201522_4103						
20110519201522_4104	2.1294	1.7363	1.3432	0.29296	0.18518	0.30956
20110519201522_4105	7.741	6.9659	6.5261	0.61219	0.57136	0.52848
20110519201522_4106	1.9494	2.2022	1.0691	0.29542	0.1663	0.17708
20110519201522_4107	7.7115	5.4744	2.876	1.5756	1.2292	0.50878
20110519201522_4108	12.565	14.711	2.839	1.5084	2.6958	0.39851
20110519201522_4110	0.7463	0.92384	0.65378	0.17708	0.13285	0.17119
20110519201522_4111	7.1557	9.9701	4.0014	1.111	1.0675	0.63866
20110519201522_4113	1.0543	1.1993	0.62622	0.25773	0.17621	0.19281
20110519201522_4115	5.1778	4.4559	2.2926	1.6102	1.047	0.49913
20110519201522_4116	11.133	10.8	3.8076	1.8852	1.899	1.2478
20110519201522_4301	33.616	25.124	10.639	1.8556	1.9138	1.1424
20110519201522_4304	91.828	104.58	67.097	3.9712	3.4213	1.8151
20110519201522_4305						
20110519201522_4306	74.804	72.785	39.437	7.9824	6.223	4.3243
20110519201522_4501	5.8179	2.9026	3.389	0.87713	0.58739	0.37642
20110519201522_4502	17.988	17.32	5.3329	2.5653	3.241	0.8904
20110519201522_4504	358.5	598.41	344.49	12.16	26.142	7.2876
20110519201522_4506	9.4919	9.852	5.3999	1.3513	1.9677	0.76448
20110519201522_5905	3.3572	3.8614	1.3043	0.64504	0.37861	0.25118
20110519201522_6401	47.847	45.572	22.672	3.7976	4.1651	1.5024
20110519201522_7701	2.495	2.9514	1.1813	0.086799	0.059756	0.023225
20110519201522_7702	18.603	7.4495	4.5585	0.95672	0.71781	0.68174
20110519201522_8103	1.684	0.92206	0.52644	0.20857	0.18843	0.12517
20110519201522_8104	1.135	1.2117	0.71321	0.33416	0.34571	0.15782
20110519201522_8105	0.7688	0.77737	0.41052	0.15075	0.11172	0.11116
20110519201522_4102	1.5136	1.389	0.6461	0.20995	0.2368	0.23376

Record Names	Processed PGA_EW (cm/s^2)	Processed PGA_NS (cm/s^2)	Processed PGA_UD (cm/s^2)	Processed PGV_EW (cm/s)	Processed PGV_NS (cm/s)	Processed PGV_UD (cm/s)
20110519201522_8107	2.2811	2.2998	1.0179	0.52181	0.58098	0.32134
20110519201522_8108	0.62946	0.83497	0.47375	0.13207	0.13388	0.09788
20110519201558_3523	2.9222	2.3968	1.3462	0.3379	0.31193	0.19621

PGA: Peak ground acceleration
PGV: Peak ground velocity

Table 3

Record Names	Station Code	Station Latitude	Station Longitude	V_{S30}	R_{epi} (km) GCMT	R_{hyp} (km) GCMT	Rjb (km) GCMT	Rrup (km) GCMT
20110519201522_0302	302	38.0599	30.15373	198.124	152.086	152.558	146.024	146.764
20110519201522_0905	905	37.85997	27.26501	369.273	212.606	212.944	207.771	208.292
20110519201522_0910	910	37.84548	27.79956		182.034	182.43	177.965	178.572
20110519201522_1006	1006	40.33193	27.99662	320.999	161.7	162.144	155.687	155.963
20110519201522_1009	1009	39.57798	28.63232	560.738	62.074	63.2233	56.0142	56.7784
20110519201522_1014	1014	40.11399	27.64236	397.238	163.975	164.413	157.908	158.18
20110519201522_1102	1102	39.90433	30.05292	401.788	119.109	119.712	114.606	114.982
20110519201522_1601	1601	40.22566	29.07518	249.065	120.721	121.316	116.364	116.733
20110519201522_1607	1607	40.39437	29.09803	176.297	139.488	140.003	135.183	135.501
20110519201522_1608	1608	40.41049	29.17928	366.155	141.527	142.034	137.437	137.751
20110519201522_1609	1609	40.42539	29.16658	228.732	143.12	143.622	138.993	139.303
20110519201522_1613	1613	39.91509	29.23167	412.393	87.1622	87.9844	83.5532	84.0674
20110519201522_1614	1614	40.03471	28.39392	264.93	115.559	116.181	109.638	110.031
20110519201522_1615	1615	40.42236	29.2907	348.691	143.724	144.224	139.94	140.247
20110519201522_1616	1616	40.44975	29.25875	571.79	146.436	146.927	142.55	142.852
20110519201522_1617	1617	40.49411	29.2993	1597.729	151.73	152.204	147.933	148.224
20110519201522_1618	1618	40.35095	28.92815		135.276	135.807	130.533	130.863
20110519201522_2008	2008	37.80916	28.8599		149.218	149.699	145.457	146.2
20110519201522_2009	2009	37.91337	29.03804		136.444	136.971	132.211	133.027
20110519201522_2011	2011	37.73719	29.1006		155.996	156.457	151.586	152.299
20110519201522_2601	2601	39.81367	30.52844	237.086	145.14	145.635	139.743	140.051
20110519201522_2602	2602	39.78929	30.49728	328.37	141.472	141.98	136.056	136.372
20110519201522_2603	2603	39.88012	30.45341	630.991	143.716	144.216	138.524	138.835
20110519201522_2604	2604	39.77329	30.51008	248.292	141.536	142.044	136.079	136.395
20110519201522_2605	2605	39.723	30.533		140.622	141.133	135.056	135.374
20110519201522_2607	2607	39.81749	30.146	279.6	118.513	119.119	113.598	113.977

Record Names	Station Code	Station Latitude	Station Longitude	V_{S30}	R_{epi} (km) GCMT	R_{hyp} (km) GCMT	Rjb (km) GCMT	Rrup (km) GCMT
20110519201522_2610	2610	39.822	30.42164		137.872	138.393	132.594	132.919
20110519201522_2611	2611	39.78828	30.44295		137.423	137.946	132.055	132.381
20110519201522_2613	2613	39.79357	30.5397		144.85	145.346	139.406	139.715
20110519201522_2614	2614	39.75347	30.55575		143.909	144.408	138.38	138.691
20110519201522_2615	2615	39.74031	30.65213		150.603	151.081	144.988	145.285
20110519201522_2616	2616	39.7063	30.61889		146.413	146.904	140.764	141.07
20110519201522_3202	3202	37.78385	30.56536		198.652	199.014	192.569	193.13
20110519201522_3405	3405	40.91	29.16		196.933	197.298	192.71	192.933
20110519201522_3406	3406	41.02	29.16		209.157	209.501	204.922	205.132
20110519201522_3409	3409	41.02651	28.75884		211.542	211.882	206.658	206.866
20110519201522_3410	3410	41.17189	29.60816		230.35	230.662	226.873	227.063
20110519201522_3503	3503	39.0739	26.88834	193.193	189.243	189.623	183.163	183.753
20110519201522_3506	3506	38.39443	27.08211	770.687	192.025	192.399	186.331	186.912
20110519201522_3510	3510	38.409	27.043		194.389	194.759	188.663	189.236
20110519201522_3511	3511	38.4213	27.2563		177.129	177.535	171.488	172.118
20110519201522_3512	3512	38.4009	27.1516		186.284	186.67	180.615	181.213
20110519201522_3514	3514	38.4762	27.1581		182.149	182.544	176.396	177.009
20110519201522_3515	3515	38.4649	27.094		187.751	188.135	181.985	182.579
20110519201522_3517	3517	38.3756	27.1936		184.329	184.72	178.713	179.318
20110519201522_3518	3518	38.4312	27.1435		185.426	185.813	179.717	180.319
20110519201522_3519	3519	38.4525	27.1112		186.959	187.344	181.213	181.81
20110519201522_3520	3520	38.478	27.2111		177.876	178.28	172.143	172.771
20110519201522_3521	3521	38.46792	27.07636		189.017	189.398	183.241	183.831
20110519201522_3522	3522	38.4357	27.1987		180.885	181.282	175.196	175.813
20110519201522_3524	3524	38.4969	27.1073		185.258	185.647	179.463	180.065
20110519201522_3525	3525	38.3723	27.1084		191.082	191.458	185.426	186.009
20110519201522_3530	3530	38.45302	27.22444		178.024	178.428	172.327	172.954
20110519201522_2610	2610	39.822	30.42164		137.872	138.393	132.594	132.919

Record Names	Station Code	Station Latitude	Station Longitude	V_{S30}	R_{epi} (km) GCMT	R_{hyp} (km) GCMT	Rjb (km) GCMT	Rrup (km) GCMT
20110519201522_4102	4102	40.78463	30.02649	999.947	199.872	200.232	197.085	197.304
20110519201522_4103	4103	40.78577	30.02504	999.947	199.938	200.298	197.156	197.374
20110519201522_4104	4104	40.68038	29.96998	769.756	187.346	187.73	184.554	184.787
20110519201522_4105	4105	40.67441	29.96935	276.854	186.719	187.104	183.92	184.154
20110519201522_4106	4106	40.78627	29.45003	701.075	185.753	186.14	182.166	182.402
20110519201522_4107	4107	40.76025	29.93246		194.263	194.633	191.63	191.855
20110519201522_4108	4108	40.76023	29.93293		194.276	194.646	191.643	191.868
20110519201522_4110	4110	41.0691	30.1525		233.089	233.398	230.369	230.556
20110519201522_4111	4111	40.6844	29.5888		177.127	177.533	173.931	174.179
20110519201522_4113	4113	40.7768	29.7335		190.334	190.712	187.391	187.621
20110519201522_4115	4115	40.74328	29.78015		188.002	188.384	185.2	185.432
20110519201522_4116	4116	40.71956	29.86583		187.984	188.367	185.36	185.592
20110519201522_4301	4301	39.42779	29.99155	266.6	84.7292	85.5747	78.9595	79.5035
20110519201522_4304	4304	38.99478	29.4004	343.222	32.0292	34.2034	26.2423	28.7849
20110519201522_4305	4305	39.09282	28.97848	259.026	10.2094	15.7554	5.46998	14.1375
20110519201522_4306	4306	39.33612	29.24905		26.2209	28.8364	22.9608	24.7668
20110519201522_4501	4501	38.61259	27.38138	340.322	158.302	158.756	152.48	153.188
20110519201522_4502	4502	38.91121	27.82326	291.714	111.501	112.145	105.48	106.501
20110519201522_4504	4504	39.03503	28.64812	335.814	39.0593	40.8611	33.1475	36.2672
20110519201522_4506	4506	38.48311	28.12347	272.932	110.47	111.12	105.643	106.663
20110519201522_5905	5905	40.98205	27.54794		242.794	243.091	236.831	237.013
20110519201522_6401	6401	38.67128	29.40401	285.498	59.1815	60.3859	53.3267	55.32
20110519201522_7701	7701	40.56416	29.30603	388.434	159.53	159.981	155.717	155.993
20110519201522_7702	7702	40.58997	29.2668	357.769	162.016	162.459	158.094	158.366
20110519201522_8103	8103	40.786	31.282		262.124	262.399	257.522	257.69
20110519201522_8104	8104	40.86109	31.18043		261.966	262.241	257.552	257.72
20110519201522_8105	8105	40.90278	31.15198		263.707	263.98	259.374	259.54
20110519201522_4102	4102	40.78463	30.02649	999.947	199.872	200.232	197.085	197.304

Record Names	Station Code	Station Latitude	Station Longitude	V_{S30}	R_{epi} (km) GCMT	R_{hyp} (km) GCMT	Rjb (km) GCMT	Rrup (km) GCMT
20110519201522_8107	8107	40.83864	31.11286		256.244	256.525	251.871	252.042
20110519201522_8108	8108	40.86128	31.23002		264.883	265.155	260.422	260.587
20110519201558_3523	3523	38.3282	26.7706		219.704	220.032	213.957	214.462

V_{S30}: The mean S-wave velocity of the top 30m of the soil profile
R_{epi}: Epicentral distance
R_{hyp}: Hypocentral distance
R_{JB}: Joyner-Boore distance (the closest distance from site to the vertical projection of the rupture plane)
R_{rup}: Rupture distance (the closest distance from site to the rupture plane)

Table 4. The coordinates and damage state of investigated buildings in Simav county center

Bldg No.	North (°)	East (°)	Height (m.)	Damage state
1	39.091981	28.979346	812	Heavy
2	39.092032	28.979107	812	Moderate
3	39.091917	28.979569	812	Moderate
4	39.091477	28.979393	814	Moderate
5	39.091674	28.979189	813	Moderate
6	39.092303	28.979174	811	Heavy
7	39.092167	28.979116	811	Moderate
8	39.091635	28.978852	813	Moderate
9	39.091217	28.979392	815	Heavy

Table 5. The coordinates and damage state of investigated buildings in Gökçeler village

Bldg. No.	North (°)	East (°)	Height (m)	Damage state
11	39.097515	29.028221	825	Heavy
12	39.097516	29.028910	826	Moderate
13	39.097888	29.029389	827	Moderate
14	39.098478	29.029456	830	Moderate
Mosque	39.098822	29.030010	830	Moderate

Table 6. The coordinates and damage states of the investigated buildings in Esenevler building complex

Bldg. No.	North (°)	East (°)	Height (m)	Damage state
A-Block	39.084181	29.009219	846	Light
B-Block	39.083885	29.008451	847	Light
C-Block	39.083611	29.009335	846	Light
“Sayar ve Peker” Apt.	39.084671	29.009039	846	Light